



## Chemical profiling of polyphenols in *Thunbergia alata* and in silico virtual screening of their antiviral activities against COVID-19

Fatma S. Abd El -Aal <sup>\*1</sup>, Hala Sh. Mohammed<sup>1</sup>, Mona H. Ibrahim<sup>2</sup> and Lotfy D Ismail<sup>3</sup>

<sup>1</sup>Department of Pharmacognosy, Faculty of Pharmacy (Girls), Al-Azhar University, Cairo, Egypt

<sup>2</sup>Department of Pharmaceutical Chemistry, Faculty of Pharmacy (Girls), Al-Azhar University, Cairo, Egypt

<sup>3</sup>Department of Pharmacognosy, Faculty of Pharmacy (Boys), Al-Azhar University, Cairo, Egypt

\*Correspondence: E-mail: [fs92020@gmail.com](mailto:fs92020@gmail.com)

Article history: Received 2021-04-18

Revised 2021-05-02

Accepted 2021-05-22

**Abstract** A comprehensive analysis of the polyphenols constituents found in *Thunbergia alata* leaves using (UPLC-Triple TOF-MS/MS) and natural polyphenols' antiviral properties have motivated us to perform in silico binding affinity study of flavonoids and coumarins identified in *T. alata* leaves extract against different proteins of SARS-COV-2; (Mpro) main protease (PDB ID: 6LU7) and 2'-O-methyltransferase (PDB ID: 6wkq) using a co-crystallized ligands N3 and Sinefungin respectively. 30 compounds were tentatively identified in *T. alata* leaves extract by UPLC-Triple TOF-MS/MS and characterized as 8-phenolic acids; 12-flavonoids; 3- coumarins and remain compounds unidentified. In silico virtual screening of both flavonoids and coumarins as the most common classes of polyphenols; flavonoids have the best potential to act as COVID-19 Mpro & MTase inhibitors; especially Kaempferol-3-O-(6''-p-coumaroyl)-glucoside; Comp. (17) which gave very best docking score { -9.2 kcal/mol} (docking energy score of N3 -7.6 kcal/mol). It bind by nine hydrogen bonds (with TRY54, CYS145, GLN192, PHE140, LEU141, THR26, ARG188 and ASN142), and Pi-Sulfur interaction (with MET165), hydrophobic interactions via five Pi-Alkyl bond (with MET49, CYS145 and PRO168) and also scored energy binding -10.2 (docking energy score of Sinefungin -7.8 kcal/mol); formed H- bond with ASN6841, ASN6899, CYS6913, LYS6968, GLY6869, GLY6871, ASP6928, ASN6996 and TRY6930. Moreover, 17 binds with LYS6844, LYS6935, LEU6898 and CYS6913 via hydrophobic interactions. While coumarins in comparison with the current flavonoids had less energy binding score. However, further research is important to investigate their potential medicine value.

**Key words:** *Thunbergia*, COVID -19, Docking, Polyphenolics, UPLC-QTOF-ESI -MS/MS; Antioxidant

### 1. INTRODUCTION

Corona Virus Disease (COVID-19) is an RNA virus with glycoprotein spikes on its envelope show a crown-like appearance <sup>(1)</sup>. It is not the primary time a coronavirus has caused an epidemic: in November 2019, a plague of coronaviruses (CoVs) with the intense acute respiratory syndrome (SARS)- CoV began within the Chinese province of Guangdong, and in September 2012, the center East respiratory syndrome (MERS)-CoV emerged <sup>(2)</sup>, (CoVs) are divided into four genera: (I) -coronavirus alpha CoV), (II) coronavirus (beta CoV), and (III) - coronavirus (delta CoV), and (IV) -coronavirus (gamma CoV), which are most likely found in bats and rodents <sup>(3)</sup>. A variety of active phytochemicals have been found to have genetically and functionally diverse therapeutic applications against the virus. The antiviral mechanism of those agents is often explained by their antioxidant activity, their scavenging capabilities, DNA inhibition, RNA synthesis, or inhibition of viral reproduction.

Numerous epidemiological and experimental studies have proven that antiviral actions work against a large number of phytochemicals <sup>(4)</sup>. Polyphenols are one of the most abundant phytochemical constituents. They are known as phenolic acids, flavonoids, coumarins, lignans, stilbenes, and other compounds based on their chemical structure. Because of their molecular structures, they can be found in almost all plants and have a high antioxidant capacity. Polyphenols also possess a wide array of beneficial pharmacological activity. They are currently widely used to treat cancer, diabetes, cardiovascular disease, arthritis, neurodegenerative disorders, and a variety of other diseases <sup>(5)</sup>. *T. alata* is an herbaceous vine belonging to family Acanthaceae is one of natural plants cultivated in Egypt rich with polyphenols, Traditional medicine employs *T. alata* as fresh root extract is used as a tonic and aphrodisiac in India. Back and knee pains, eye inflammation, piles, and some ear disorders in cattle are all treated with this plant medicinally <sup>(6)</sup>. *T. alata* leaves have been shown to be used

to treat boils and other skin problems <sup>(7)</sup>.

This plant's leaf powder has anti-inflammatory effects. <sup>(8)</sup>, the whole plant extract have the hypoglycemic activity <sup>(9)</sup> and the anti-bacterial activity against *Salmonella typhi* and *Pseudomonas aeruginosa* was reported <sup>(10)</sup> in spite of vast body of research concerning *T. alata* leaves, its antiviral activities is not clear. Thus, the study aims to use ultra-performance liquid chromatography coupled by mass spectrometry (UPLC-MS/MS) to recognize polyphenolic constituents in *T. alata* leaves, as well as in silico screening of their antiviral activities against COVID-19.

## 2. METHODS

### 2.1 Collection, identification and drying of Plant materials

Fresh leaves of *Thunbergia alata* were collected from the Attia Shoala flower plantation in Kaliobeya, Egypt during May and June (2018) (flowering stage). The plant was kindly identified by Dr. Therese Labib, Botanical specialist, department of Flora and Taxonomy, El-Orman Garden, Giza, Egypt. A voucher specimen (Reg. No. T5) of the plant was deposited in the pharmacognosy department's herbarium at Al- Azhar University's Faculty of Pharmacy in Cairo, Egypt.

### Preparation of plant extract

Maceration of air-dried powder (50g) in 70% ethanol. (3x500ml) at (25±2) °C., the extract was filtered, and the solvent was evaporated using a rotary evaporator (Buchi Co., Switzerland) at 50 °C. To obtain 100mg semi-dried extract for chemical profiling.

### 2.2. UPLC-QTOF-MS/MS

UPLC-QTOF-MS/MS was accustomed to investigate the secondary metabolites of *T. alata* leaves extract. The temperature of the LC system was set to room temperature. In 1 mL of mobile phase A (5 mM HCOONH<sub>4</sub> buffer at pH8 in 1% methanol), 50 mg of extract was dissolved., vortexed for 2min followed by ultra-sonication for 10min, centrifugation for 5min at 10000rpm phase then 20µl stock(50/1000µl) re diluted with 1000 µl reconstitution solvent. Finally, the injected concentration was 1µg/µl. The following multi-step linear gradient was applied mobile phase A (5 mM HCOONH<sub>4</sub> buffer pH8 in 1% methanol) with gradient increase from (10-90) % of mobile phase B. (100 % acetonitrile) for 28 minutes with a rate of flow 0.3 ml/min. Columns; pre column In-Line filter disks 0.5 µm x 3.0 mm (Phenomenex), column X select HSS T3

2.5 µm, 2.1x150 mm (waters) Column temperature 40

°C were used for separation. Analyst software TF 1.7.1 (SCIEX) for LC-QTOF control, the injection volume in the UPLC system was 15 µL for sample and mobile phase as the blank sample.

## 3. RESULTS

### 3.1 UPLC-QTOF-ESI-MS/MS of polyphenolic compounds

In the current study, the polyphenolic 2<sup>nd</sup> metabolites in *T. alata* leaves ethanol extract were identified using UPLC-QTOF-ESI-MS/MS. The RT, full MS spectra, and MS<sup>n</sup> were used to determine the limit of detection for each peak of Compounds. By comparing reference compounds spectra and literature, fragmentation patterns in negative mode were revealed. 30 comps were identified tentatively in *T. alata* extract and characterized as phenolic acids; Caffeic acid (1), 3,4-Dihydroxybenzoic acid (2), 4-Hydroxy-3-methoxy mandelate (3), Chlorogenic acid (4), Rosmarinic acid (7), Phlorizin (8), Astringene (16) & p-coumaroylmalic acid (28). Flavonoids Daidzein-8- C-glucoside (6), Kaempferol- 3-O-Lrhamnoside (10), Baicalein-7-O-glucouronouide (11), Datiscin (12), Formononetin (13), Apigenin-7-O-glucoside (15), 4'-hydroxyisoflavone-7-O-glucoside (20), Kaempferol-7- neohesperidoside (26), 3'-Methoxy-4',5,7-trihydroxy-flavone (27), Myricetin (29) and Isorhamnetin-3-O rutinoid (30). Coumarins; Scopoletin (14) Delphinetin (19) and Esculin (23). Fatty acid; Gamma Linolenic acid (25). [ **Figure 1 & Table 1**].

### 3.2. Molecular Docking

All docked molecules were established to be anchored closely in the active binding site of main protease (Mpro) and (2') O-RNA methyltransferase (MTase) enzymes of SARS-CoV-2 with range of binding energies (-5.4 to -9.2) kcal/ml and (-6.1 to -10.2,) kcal/mol, respectively (Supplementary data; **Table S**, **Figure. S1** and **S2**). Flavonoids have the best potential to act as COVID-19 Mpro & MTase inhibitors; especially Kaempferol-3-O-(6'''-p-coumaroyl)-glucoside (fig. 2, 3).

## 4. DISCUSSION

### 4.1. Annotation of polyphenolics using UPLC- QTOF-MS/MS

#### Flavonoids

Comp. 6 was detected at Rt 2.90 min, with deprotonated ion [M-H]<sup>-</sup> at m/z 415.16, it could be identified as Daidzein-8-C- glucoside (Puerarin) <sup>(11)</sup>. Comp. 10 detected at Rt 5.47min, showed a deprotonated ion [M-H]<sup>-</sup> at m/z 431.23 and MS<sup>n</sup> ions were observed at m/z 385.18, 223.13 and 153.09, it was tentatively identified as Kaempferol-3-O-L- rhamnoside <sup>(12)</sup> Comp. 11 detected at Rt 5.75min, showed a molecular weight 414g/mole. Ions were observed at m/z 415.17, 299.6, 269.04 & 179.06,

it was tentatively identified as Baicalein-7-O-glucouronide (Baicalin) <sup>(13)</sup>. Comp. 12; was detected at Rt 6.26 min, showed a deprotonated ion [M-H]<sup>-</sup> at m/z 593.16 and MS<sup>n</sup> ions were observed at m/z 549.1, 539.3, 447.10 and 285.03 which identified 431.09 and MS<sup>n</sup> ions were

observed at  $m/z$  269.04 266.03 which identified tentatively as apigenin-7- *O*-glucoside<sup>(16)</sup>, Comp. 20 was detected at  $R_t$  10.66 min, showed a deprotonated ion  $[M-H]^-$  at  $m/z$  299.21 characteristic for molecular weight 230 g/mol and MS<sup>n</sup> ions were observed at  $m/z$  266.04, 258.04 229.04, 210.08, 203.02, 146.11 and 128.06 which identified tentatively as 3, 5, 7-trihydroxy-4'- methoxyflavanone<sup>(19)</sup>. Comp. 22 was detected at  $R_t$  13.47 min, showed a deprotonated ion  $[M-H]^-$  at  $m/z$  283.06 and  $[M-2H-CH_3]$  at  $m/z$  266.03 which tentatively identified as acacetin<sup>(19)</sup>. Comp. 24 was detected at  $R_t$  15.59 min, showed a deprotonated ion  $[M-H]^-$  at  $m/z$  413.8 which characteristic for molecular weight 414 g/mole. So comp. 24 tentatively identified<sup>(20)</sup>. Comp. 29 was detected at  $R_t$  23.20 min, showed a deprotonated ion  $[M-H]^-$  at  $m/z$  317.12, and MS<sup>n</sup> ions were observed at  $m/z$  248.9, 180.9 and 116.6 which tentatively identified as myricetin<sup>(21)</sup>.

### Coumarins

Comp. 14 was detected at  $R_t$  7.44 min, showed a deprotonated ion  $[M-H]^-$  at  $m/z$  191.02 and MS<sup>n</sup> ions were observed at  $m/z$  175.90 and 131.01 which tentatively identified as Scopoletin<sup>(22)&(14)</sup>. showed a deprotonated ion  $[M-H]^-$  at  $m/z$  177.05 and MS<sup>n</sup> ions were observed at  $m/z$  162.03 145.02 5.03 131.01 121.02 118.04 117.03 which tentatively identified as Daphnetin (7,8-Dihydroxycoumarin)<sup>(23)</sup>. **Comp. 23** was detected at  $R_t$  14.71 min, showed a deprotonated ion  $[M-H]^-$  at  $m/z$  339.08 and MS<sup>n</sup> ions were observed at  $m/z$  293.21, 177.0 and 149.0 which tentatively identified as **Esculin** (6,7-Dihydroxycoumarin 6-glucoside)<sup>(24)</sup>.

## 4.2. Molecular Docking

The Protein Data Bank (<https://www.rcsb.org/>) was used to obtain the crystal structures main protease of COVID-19 (Mpro) (PDB ID: 6LU7)<sup>(25)</sup>. And 2'-O-methyltransferase (PDB ID: 6wkq)<sup>(26)</sup>. Autodock Vina 4.2 was used to perform the docking study, which requires both the ligand and the receptor to be in pdbqt extension. Prior to the docking, M.G.L were the tools used for preparing the two enzymes, as well as the co-crystallized and two lead compounds, in the proper format<sup>(27)</sup>. By re-docking the co-crystallized ligands into their complexed enzymes, the measured RMSD between the docked and co-crystallized ligands was less than 0.67 Å, suggesting that the docking method was valid. The docking results were visually inspected using the Discovery Studio 4.5 visualizer<sup>(28)</sup>.

### 4.2.1. Docking into main protease of COVID-19

Various research groups have focused into the (Mpro) of SARS-CoV-2, also known as 3CLpro (chymotrypsin-like protease, as a possible drug target to treat COVID-19. It is essential for replication of RNA viruses because it aids in the translation and maturation of viral RNA, providing it an engaging target for drugs

against coronavirus<sup>(29)</sup>. 3CLpro composed of 9  $\alpha$ -helices and 13  $\beta$ -strands, with 3 distinct domains (Domain I, II, III) with an extended loop. The catalytic dyad of the SARS-CoV-2 virus consists of conserved amino acid residues CYS145 and HIS41, and the determination of binding site of substrate is created by splitting Domain I and II<sup>(30)</sup>. All docked molecules were established to anchored closely in the active binding site of COVID-19 3CLpro with range of binding energies (-5.4 to -9.2) kcal/mol (Supplementary data). The flavonoids act as a protease inhibitor especially Comp. (17) which showed the highest docking score -9.2 kcal/mol It formed nine H-bonds (with TRY54, CYS145, GLN192, PHE140, LEU141, THR26, ARG188 and ASN142), and Pi Sulfur interaction (with MET165), in addition to hydrophobic interactions via five Pi Alkyl bond (with MET49, CYS145 and PRO168) **Fig. 2**. On the other hand, N3 formed seven hydrogen bonds (with CYS 145, GLN 189, THR26 and HIS 163), Pi-Anion with GLU166, Pi-Sigma with HIS 41 and two alkyl interactions with MET49 and MET165 **fig. 2**. Additionally, there were another eight flavonoid comp.s with lower binding energy than the native ligand in binding affinity ranged from - 7.8 kcal/mol (comp.s 18 and 6), -7.9 kcal/mol (comp. 24), -8.1 kcal/mol ( comp. 15 ), -8.2 kcal/mol (comp. 11), - 8.3 kcal/mol ( comp. 10), -8.7 kcal/mol (comp. 12) and - 8.9 kcal/mol (comp. 29 ). Whereas the coumarin comp.s 14, 19 and 23 observed that has less energy binding equal -5.4, -5.9 and -7.2 respectively to conclude that coumarins less protease inhibitor than flavonoids (**Figure. 2** and supplementary data).

### 4.2.2. Docking into SARS-CoV- 2- (2') O RNA methyltransferase (MTase);

A potential target for antiviral therapy is (MTase) which is needed for formation of RNA cap, that required for stability of viral RNA<sup>(31)</sup>. It belongs to a large class of SAM-dependent methyltransferases, this MTase feature is binding to the nsp-16 protein, that needs a co-factor nsp-10, to function properly. ASP6928, LYS6839, LYS6968, and GLU7001 are highly conserved residues in protein nsp-16 that form the catalytic canonical motif (K-D- K-E) conserved among class I MTases<sup>(32)</sup>

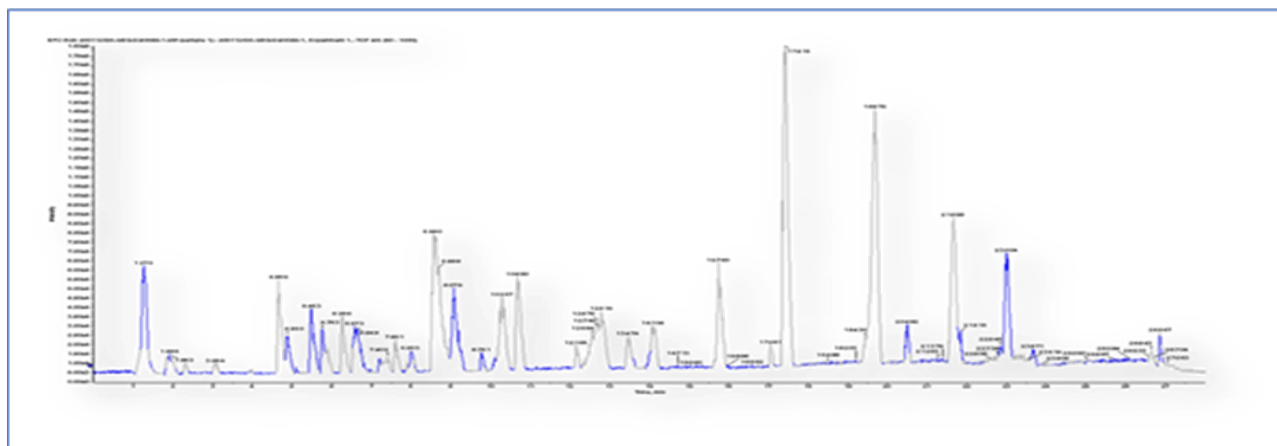


Figure (1): Negative mode UPLC-QTOF-ESI-MS/MS chromatogram of leaves. Peak numbers agree with those in Table (1).

Table (1): Tentatively identified polyphenol comp.s by negative mode UPLC-QTOF-MS/MS in *T. alata* leaves ethanolextract.

No	RT	[M-H] <sup>-</sup>	Major product ions (m/z)	Tentatively identified compounds
1.	1.23	179.03	Not fragmented	Caffeic acid
2.	1.24	153.02	109.03, 98.79	3,4-Dihydroxybenzoic acid
3.	1.31	197.03	151.06, 137.02, 122.03	4-Hydroxy-3-methoxymandelate
4.	1.90	353.09	288.03, 207.05, 199.80, 179.03	Chlorogenic acid
5.	1.97	346.10	189.06, 181.08	Unidentified
6.	2.90	415.16	Not fragmented	Daidzein-8-C-glucoside
7.	4.65	359.07	197.6, 179.03, 161.02, 133.02	Rosmarinic acid
8.	4.87	435.10	Not fragmented	Phlorizin
9.	5.47	345.15	Not fragmented	Unidentified
10.	5.47	431.23	285.18, 223.13, 153.09	Kaempferol-3-O-L-rhamnoside
11.	5.75	445.17	415.17, 299.60, 269.04, 179.06	Baicalein-7-O-glucouronide
12.	6.26	593.16	549.10, 539.30, 447.10, 285.03	Datiscin
13.	6.66	267.08	252.07, 193.10, 180.03, 155.07, 149.05 133.02	Formononetin
14.	7.44	191.02	175.90, 131.01	Scopoletin
15.	7.59	431.09	269.04, 266.03	Apigenin-7-O-glucoside
16.	8.60	405.16	225.11	Astringene
17.	9.07	593.12	309.09	Kaempferol-3-O-(6''-p-coumaroyl)-glucoside
18.	10.28	269.05	240.03, 177.06, 162.03, 159.03 145.02, 121.117.02	Apigenin
19.	10.28	177.05	162.03, 145.02, 131.01, 121.02, 118.04, 117.	Daphnetin
20.	10.66	299.21	266.04, 258.04, 229.04, 210.08, 203.02, 146.1128.06	3, 5, 7-trihydroxy-4'-methoxyflavanone
21.	12.16	467.22	399.25, 179.06, 143.03	Unidentified
22.	13.47	283.06	266.03	Acacetin
23.	14.71	339.08	293.21, 177.0, 149.0	Esculin
24.	15.59	413.80	Not fragmented	4'-hydroxyisoflavone-7-O-glucoside
25.	17.06	277.21	210.01, 151.02	gamma Linolenic acid
26.	19.86	593.14	473.11	Kaempferol-7-neohesperidoside
27.	20.49	315.21	300.04, 273.08, 269.24, 256.10 178.95, 148.	3'-Methoxy-4',5,7-trihydroxy flavone
28.	21.60	279.23	261.22	p-coumaroyl-malic acid
29.	23.2	317.12	248.90, 180.89, 116.6	Myricetin
30.	26.63	623.2	616.5	Isorhamnetin-3-O-rutinoside



Residues LEU6898, ASP6912, CYS6913, MET6928, and PHE6947 stabilize the adenosine moiety of SAM in the nsp-10-nsp-16 complex crystal structure bound to the pan- MTase inhibitor sinefungin (PDB: 6WKQ) at 2.0-Å in the active site. SAM's sugar moiety interacts with GLY6871 and ASP6897 residues, as well as two water molecules that interact with ASN6899, and the interaction of methionine moiety with ASN6841, GLY6871, ASP6928, and TYR6845. Sinefungin is in the same manner as SAM does<sup>(30)</sup>. The energy of binding is obtained from docking 6wkq with Sinefungin, compounds 14, 19, 23, 10, 17, 12, 29, 15, 22, 11, 18, 20, 24, 13, 6, and 29 were -7.8, -6.1, -6.7, -7.4, -7.7, -10.2, -8.8, -8.9, -9.5, -7.6, -8.7, -8.8, -7.3, -8.8, -8.4, -9.3 and -9.3 kcal/mol, respectively (Supplementary data). Docking analysis (Table 1) showed that all compounds fit in the correct binding site. Whereas comp. 17 showed also the highest binding score, formed H bond with ASN6841, ASN6899, CYS6913, LYS6968, GLY6869, GLY6871, ASP6928, ASN6996 and TRY6930. Moreover 17 binds with LYS6844, LYS6935, LEU6898 and CYS6913 via hydrophobic interactions. (Supplementary data, **Figure. 3**).

### 5. CONCLUSION

Flavonoids, are a wide group of polyphenolic compounds with a benzo- $\gamma$ -pyrone structure, are used to prevent and cure diseases, and have significant biological activity. Many flavonoids have been shown to be effective antiviral agents in clinical trials. Kaempferol-3-O-(6''-p-coumaroyl) - glucoside; in the current study showed the highest energy binding score to achieve the best natural antiviral remedy, so it should be interesting to separate it using chromatographic techniques and detected by authentic sample, 1D and 2D NMR spectroscopy for further in-vivo and in-vitro research as a natural antiviral remedy.

### List of abbreviations

COVID-19	Coronavirus disease
SARS-CoV-2	Severe acute respiratory syndrome coronavirus 2
3CLpro	Chymotrypsin-like protease
Mpro	Main protease
2' O-RNA MTase	(2') O RNA methyltransferase
T. alata	Thunbergia alata
UPLC-QTOF MS/MS	Ultra-performance liquid chromatography quadrupole time of flight mass spectrometry
m/z	Major product ions

### REFERENCE

1. Perlman S, Netland J, Coronaviruses post-SARS: Update on replication and pathogenesis. *Nat Rev Microbiol.* 2009; 7(6): 439–450.
2. Prof Roujian Lu Ms, Xiang Zhao M, Juan Li P, Peihua Niu P Bo, Yang Ms Honglong, Wu Ms et al. Genomic characterisation and epidemiology of 2019 novel coronavirus: implications for virus origins and receptor binding. *NCBI.2020; 395(10224): 565–74*
3. Yin Y, Wunderink RG MERS, SARS and other coronaviruses as causes of pneumonia. *Resp.* 2018; Feb; 23(2):130-7.
4. Muthu B, Janarthanan AK. Antiviral activity of herbal plants and its phytochemicals (an overview) . *Mukt Shabd Jour.*2020; 2347-3150.
5. Sinha D, Pharmacological Importance of Polyphenols a Review. *Inter. Res. Jour. Of Pharmacy.* 2019. 10: 13–23.
6. Ram M, Rao K, Alam A, Singh KS, Ram M, Rao K. Preliminary phytochemical analysis of different extracts of *Ruellia patula* Luffa aegyptiaca and *Thunbergia alata*. *Chem. and Pharm. Res.* 2015; 7(10):315-20.
7. Rojas Sandoval J, Acevedo Rodriguez P. *Thunbergia alata* (black eyed Susan) [Internet]. I S C. 2018. Available from: <https://www.cabi.org/isc/datasheet/53646#tocontributor>.
8. Cho YC, Kim YR, Kim BR, Bach TT, Cho S. *Thunbergia alata* inhibits inflammatory responses through the inactivation of ERK and STAT3 in macrophages. *Vol. 38, Inter. J. of Mol. Med.* 2016: 1596–604.
9. Charles A, Ramani VA. Chemosymantics of genus *Tunbergia* *IJSRME.* 2016; 2455 – 5630:5-11.
10. KH S, S C. Ethnopharmacological and phytochemical review on *Thunbergia Retz.* (Montin.) *Species. Med Aromat Plants* 2015; 04:217
11. Jeevan K. P, Kenneth J, Marion K, Landon W, Michelle S-J, Connie W Profiling and Quantification of Isoflavonoids in Kudzu Dietary Supplements by HPLC and ESI-TMS. *2 J. Agric. Food Chem.* 2003; 51(15): 4213-18
12. Rivière C, Hong VNT, Pieters L, Dejaegher B, Heyden Y Vander, Van MC, et al. Polyphenols isolated from antiradical extracts of *Mallotus metcalfeanus*. *Phytochemistry.* 2009; 70(1):86–94.
13. Yuan Y, Hou W, Tang M, Luo H, Chen LJ, Guan YH, et al. Separation of flavonoids from the

- leaves of *Oroxylum indicum* by HSCCC. *Chromatographia*. 2008;68 :885–92.
14. Tine Y, Renucci F, Costa J, Wélé A, Paolini J. A method for LC-MS/MS profiling of coumarins in *Zanthoxylum zanthoxyloides* (Lam.) B. Zepernich and timler extracts and essential oils. *Molecules*. 2017; 22; 22(1):174.
  15. Zhao X, Zhang S, Liu D, Yang M, Wei J. Analysis of Flavonoids in *Dalbergia odorifera* by Ultra-Performance Liquid Chromatography with Tandem Mass Spectrometry. *Molecules*. 2020; 25(2):389.
  16. Ana Plazonić, Bucar F, Maleš Ž, Mornar A, Nigović B, Kujundžić N. Identification and Quantification of flavonoids and phenolic acids in burr parsley (*caucalis platycarpus* L.), using high-performance liquid chromatography with diode array detection and electrospray ionization mass spectrometry. *Molecules*. 2009;14 :2466–90.
  17. Seon-H L, Heon-W, Min-KL, Young J K, Gelila A Y-SC et al. Phenolic profiling and quantitative determination of common sage (*Salvia plebeia* R. Euro Food Res. and Tech. 2018;244(9):1637–46
  18. María de la Luz Cádiz-Gurrea, Salvador F-A, Jorge J, Antonio S-C. Comprehensive characterization by UHPLC-ESI-Q-TOF-MS from an *Eryngium bourgatii* extract and their antioxidant and anti-inflammatory activities. 2013; 09. (38): 197–204.
  19. Sawada Y, Nakabayashi R, Yamada Y, Suzuki M, Sato M, Sakata A, et al. RIKEN tandem mass spectral database (ReSpect) for phytochemicals: A plant-specific MS/MS-based data resource and database. 2012; 82:38–45.
  20. Anna S, Barbara S, Joanna B, Dorota M MJ, MS. LC\_MS profiling of flavonoid glycoconjugates isolated from hairy roots, suspension root cell cultures and seedling roots of *Medicago truncatula* . *Metabolomics*. 2011; 7: 604–13.
  21. Venkatalakshmi P, Vadivel V, Brindha P. Identification of flavonoids in different parts of *terminalia catappa* L. Using LC-ESI-MS/MS and investigation of their anticancer effect in EAC cell line model. *Pharm.Sci.and Res*. 2016; 8: 176–83.
  22. Siwinska J, Kadzinski L, Banasiuk R, Gwizdek-Wisniewska A, Alexandre O, Banecki B, et al. Identification of QTL affecting scopolin and scopoletin biosynthesis in *Arabidopsis thaliana*. *BMC Plant Bio* .2014; 14:280.
  23. Yefchak V L. Mass Spectral Fragmentation Studies of Coumarin-Type Comp.s Using GC High-Resolution MS. *Analyt. Chem*. 2011; 5: 27-36.
  24. Ying-L, YingS C,Liu X, HuangX Z Neng L M , XuSui M N ,Sheng W. Simultaneous determination of esculetin and its metabolite esculetin in rat plasma by LC-ESI-MS\_MS and its application in pharmacokinetic study -. *J Chromatogr B Analyt Technol Biomed Life Sci* .2012 Oct 15; 907:27-33.
  25. Jin Z, Du X, Xu Y, Deng Y, Liu M, Zhao Y, et al. Structure of Mpro from SARS-CoV-2 and discovery of its inhibitors. *Nature*. 2020; 582(7811):289–93.
  26. Rosas-Lemus M, Minasov G, Shuvalova L1, Inniss NL, Kiryukhina O BJ, Satchell KJF. High-resolution structures of the SARS-CoV-2 2'-methyltransferase reveal strategies for structure-based inhibitor design. *Science Signaling* .2020; 13: 651.
  27. Oleg T, Arthur J. O. AutoDock Vina: Improving the Speed and Accuracy of Docking with a New Scoring Function, Efficient Optimization, and Multithreading. *Journal of comp. chem*. 2010; 31: 455–61.
  28. Mahmoud A. H, Tamer M. I, Sara T. R, Amal Alharbi ROE& WME. In silico identification of novel SARS-COV-2 2'-O-methyltransferase (nsp16) inhibitors\_ structure-based virtual screening,molecular dynamics simulation and MM-PBSA approaches. 2021; 36(1): 727–36.
  29. Mothay D, Ramesh K V. Binding site analysis of potential protease inhibitors of COVID-19 using AutoDock. *VirusDisease*. 2020; 31(2):194–9.
  30. Sang P, Tian SH, Meng ZH, Yang LQ. Anti-HIV drug repurposing against SARS-CoV-2. *RSC Adv*. 2020; 10(27):15775–83.
  31. Krafcikova P., Silhan J., Nencka EB R.Discovery of Neutralizing Antibody (NAb) and Peptide Targeting SARS-CoV - Creative Biolabs. 2020.
  32. Rosas-Lemus M, Minasov G, Shuvalova L, Inniss N, Kiryukhina O, Brunzelle J, et al. Structure of SARS-CoV-2 2'-O-methyltransferase heterodimer with RNA Cap analog and sulfates bound reveals new strategies for structure-based inhibitor design. *Nature*. 2020.